Design Modifications in RF Interaction Cavity of a 140 GHZ Gyrotron to Achieve Wide Tunable Bandwidth for DNP NMR Applications

Sivavenkateswara Rao V, Muthiah Thottappan, Pradip Kumar Jain

Abstract: ***The tapered RF interaction cavity of 140 GHz tunable continuous wave (CW) gyrotron operating in*** $TE_{0,3,q}$ ***mode has been tailored with the aim of providing RF power over a tunable bandwidth for 212 MHz DNP NMR spectroscopy applications. Gyrotron device RF interaction cavity design, its beam absent RF characteristics as well as electron beam and RF wave interaction behavior, both analytical and Particle-in-Cell (PIC) simulation studies have been presented. Using linear analysis, the start oscillation currents and the RF field profiles for the various axial operating modes indices q = 1, 2, 3 have been determined. Suitable modifications in the interaction cavity have been incorporated for the enhancement of device tunable bandwidth by operating the gyrotron in the high order axial indices via magnetic tuning. Gyrotron beam-wave interaction behaviour explored using time dependent non-linear multi-mode analysis for various beam currents and magnetic fields and more than >15W of RF power over a tunable bandwidth of 400MHz has been achieved through magnetic field tuning. This tunable bandwidth gyrotron design will of immense use for enhancement of sensitivity of the DNP NMR spectroscopy.***

Keywords: Beam wave interaction, CRM instability, DNP NMR applications, Tunable gyrotron oscillator.

I. INTRODUCTION

Gyrotron is a high power high frequency microwave source which works on the principle of CRM instability and generates power of several kW to few MWs in millimeter and sub-millimeter frequency range. It is one class of fast wave device where the phase velocity of the RF wave is comparable with the velocity of light in free space. Gyrotrons widely used in various applications like Electron Cyclotron Resonance Heating, Electron cyclotron Current Drive, material processing which requires very high power of several kW to few MW at higher frequencies [1-4]. Besides high RF power generations at single or step tunable frequencies, it is suitable to generate a low power level of few watts to tens of watts over a band of frequencies in the millimeter and submillimeter regime. Dynamic Nuclear polarization (DNP) is a key technique which transfers unpaired electrons spin polarization into nuclear spins and is used for the enhancements of sensitivity of Nuclear Magnetic Resonance (NMR) spectroscopy study that enables faster data acquisitions in various sample characterization.

Revised Manuscript Received on October 30, 2019.

Sivavenkateswara Rao V, Centre of Research in Microwave Tubes, Department of Electronics Engineering, Indian Institute of Technology (Banaras Hindu University), Varanasi-221005, India.

M.Thottappan, Centre of Research in Microwave Tubes, Department of Electronics Engineering, Indian Institute of Technology (Banaras Hindu University), Varanasi-221005, India.

Pradip Kumar Jain, Department of Electronics and Communication Engineering, National Institute of Technology, Patna 800005, India.

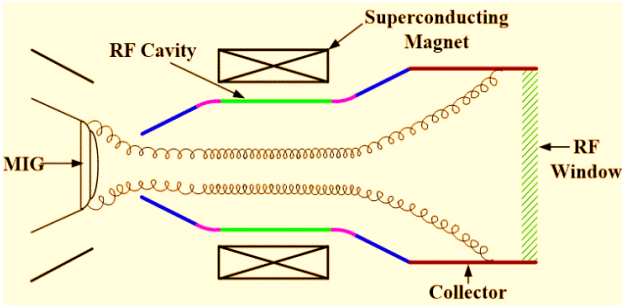

Fig. 1: Typical schematic of a tapered gyrotron oscillator [3].

By incorporating the DNP technique in NMR spectroscopy, the enhancement in sensitivity factor is ≈ 660. For the successful enhancement of sensitivity study by DNP technique NMR spectroscopy, an RF source is needed that able to operate at the NMR frequencies. In addition to this, the NMR spectroscopy requires either a super conducting NMR magnet with sweep coils or a tunable RF source for the study of various samples characterization. Due to the complexities involved in the

arrangements and maintenance of a tunable NMR magnet, the focus has been shifted on the development of tunable RF microwave sources at various NMR frequencies [5-6].

Gyrotron oscillator is the most suitable RF source for this application. Fig.1 shows a typical schematic of the cylindrical tapered RF cavity gyrotron oscillator where the extraction of RF power in the axial direction. The radial extraction can be also be achieved by placing an internal quasi optical mode converter after RF cavity that eases the collector design simple and more reliable. Gyrotron consists of magnetron injection gun (MIG) operating under temperature limited region generates a gyrating electron beam which is guided by the external axial DC magnetic field. The electron beam then enters into the interaction region, i. e., RF cavity, where it interacts with the RF waves and exchanges its energy to the RF waves. In this device, the kinetic energy of the electrons is transferred into RF energy through azimuthal bunching. A nonlinear taper section acts as impedance matching section between the cavity and the collector and transport out the RF energy with much lower background DC magnetic field and spent electrons are collected at the collector while the RF wave travels through collector and exits through vacuum window.

In Gyrotrons, the main interaction mode is the transverse electric ($TE_{m,p,q}$) mode where m indicate number of full wave variations in azimuthal direction, p indicates the number of half wave variations in the radial direction and q indicates number of peaks in the axial direction. In case of high power gyrotrons, the value of axial mode number is always 1 but for low power tunable gyrotrons, usually q varies from 1 to 6, there by achieving a minimum threshold power over a continuous frequency range without variation of m and p indices of the mode. This allows us to design the after cavity components simple. For this, longer cavities are usually incorporated in the low power, tunable gyrotrons.

Various low power tunable gyrotrons operating at 140 GHz, 250 GHz, 263 GHz, 330 GHz and more have been implemented and tested experimentally [1, 5-7]. In the present work, an experimentally demonstrated low power gyrotron operating with beam voltage 12.3 kV and current 25mA at 140 GHz for 212 MHz DNP NMR spectroscopy reported by Colin D Joyce *et al.* is revisited and its RF cavity design is suitably modified to enhance device tunable bandwidth by magnetic tuning [7]. With the reported RF cavity geometry as well beam parameters, the RF analysis and the beam wave interaction behaviour is studied using nonlinear multimode theory as well through PIC simulation using a commercial PIC code "CST Studio Suite" [8-11]. Since the reported gyrotron has a limited tunable bandwidth via magnetic tuning and only thermal tuning has been used [7]. With the aim of achieving wider device tunable bandwidth, the tapered cylindrical RF interaction cavity is suitably modified such that in addition to thermal tuning, the magnetic tuning can also be achieved by operating the device in the high order axial operating modes using the same beam parameters. The operating mode is considered here as $TE_{0,3,q}$ with a target of more tunable bandwidth through magnetic tuning as well. With the modified RF cavity, the cold cavity analysis and its electron-beam and RF-wave interaction behaviour studies through analysis as well as PIC simulations at various beam currents and magnetic fields are carried out.

In section II, the cold cavity analysis and the start oscillation current I_{soc} curves that provide information for the state of the mode oscillation at various magnetic fields are presented. Followed by the determination of RF field profiles, quality factor and resonant frequency calculations under beam absent conditions are derived for the Colin D Joyce *et al.* cavity and the modified cavity. The beam wave interaction mechanism in the RF cavity under various modes is studied using time dependent, non-linear, multimode theory and the same is also validated through PIC simulation code of Commercially CST Studio Suite results in Section III. Followed by a conclusion that summarizes the presented research work at end.

II. RF INTERACTION CAVITY DESIGN AND ANALYSIS

A RF source generates the RF energy by interacting with DC electron beam. Suitable environments are required for the successful RF generations with desired characteristics that include selection of appropriate beam parameters, and the space that allows the interaction between electron beam and RF wave i.e. Interaction region.

A conventional, tapered cylindrical RF interaction cavity is taken as an interaction region in the present design and its 2Dimensional axis symmetric view is shown in Fig. 2. The RF cavity mainly consists of three sections, first a down taper section of length L_d, of an angle θ_d provides shielding

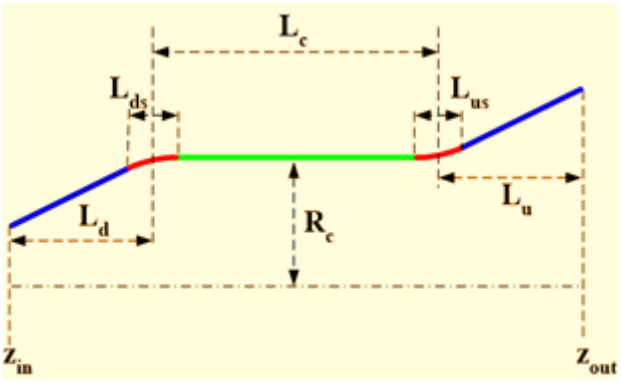

Fig. 2: 2D axis symmetric view of the cylindrical tapered RF interaction cavity of the gyrotron [4].

for back wave propagation towards the gun, followed by a uniform middle section acts as effective interaction space, where active beam-wave interaction takes place, of length L_c and ended by an up-taper section where the RF standing waves get converted into travelling waves to extract out RF energy, of length L_u with angle θ_{up}. Usually, parabolic smoothing section of lengths L_{ds} and L_{us} at down-taper and up-taper transitions, respectively, are used to minimize the mode conversions and these sections becomes significant where the short interaction cavity regions and the high taper angles of cavities [3, 4]. Based on the operating mode and frequency of operation, the plausible interaction cavity radius R_c and electron beam radius R_b of the gyrotron are given by [3, 4]:

$$R_c = \frac{\chi_{mp}\lambda}{2\pi} = \frac{\chi_{mp}c}{2\pi f_c} \quad , \qquad (1)$$

and

$$R_b = \frac{\chi_{m\pm s,i}R_c}{\chi_{mp}} = \frac{\chi_{m\pm s,i}\lambda}{2\pi} = \frac{\chi_{m\pm s,i}c}{2\pi f_c} \quad . \qquad (2)$$

Here χ_{mp} is the p^{th} root of m^{th} order Bessel function $J'_m(x) = 0$, c is the velocity of light in free space, f_c is the frequency of operation, s is the harmonic number and i indicates the number of maximum radial position of the field where the beam is to be launched in the interaction structure.

Design and optimization of an RF interaction cavity requires knowledge of axial RF field profiles $V_{mp}(z)$, resonating frequencies f_{res}, and its diffractive quality factor Q_{diff} that gives the information about the amount of RF power diffracted from cavity.

For the mild taper angles ($<10^0$), by employing the single mode Vlasov approximation where only single $TE_{m,p}$ mode is retained in the expansion of coupled equations and coupling due to the other modes are neglected. Therefore, in single mode approximation, the RF field profile $V_{mp}(z)$ in the interaction structure can be given by [4]:

$$\frac{d^2V_{mp}}{dz^2}+\left(\frac{\omega^2}{c^2}-k_{mp}^2(z)\right)V_{mp}\simeq+i\omega J_{mp}, \qquad (3)$$

where $J_{mp}=\int d\phi\int_0^{R_c}\mathrm{Re}^*_{mp}.JdR.$ is the source term, the complex RF frequency $\omega=\omega_{res}\left(1+i/2Q_{diff}\right)$, ω_{res} resonant frequency and the transverse wave number.The functions $V_{mp}(z)$ must satisfy radiation boundary conditions at the ends of the interaction cavity and can be written as:

$$\left.\frac{dV_{mp}}{dz}\right|_{z_{in}}=ik_z(z_{in})V_{mp}(z_{in}),$$
$$\left.\frac{dV_{mp}}{dz}\right|_{z_{out}}=-ik_z(z_{out})V_{mp}(z_{out}). \qquad (4)$$

Here, k_z is the axial wave number and given by $k_z(z)=\sqrt{(\omega/c)^2-k_{mp}^2(z)}$, z_{in} and z_{out} indicates the down taper and up taper axial ends of the interaction structure respectively. The solutions to the coupled equations are carried out with the Numerov's algorithm, a reputed numerical method when the source term is set as: J_{mp}=0 [12].

Generally, for broadband tunable gyrotrons, it is advantageous to design the RF cavity which operates in the mode over a range of frequency i.e., $TE_{m,p,q}$, where the axial mode index q changes usually from 1,2,3 etc. This kind of implementation eases the design of the post RF interaction cavity components i.e., nonlinear taper, collector and the RF window for the collecting and guiding the generated RF power simpler. Usually a longer interaction cavity section is chosen and L_c is of few tens of wavelengths for the smooth transitions over axial mode indices as frequency varies. Longer interaction cavities yield higher Q values. The diffractive quality factor $Q_{diff,q}$ for the various axial mode indices are related to fundamental $Q_{diff,1}$ as [8-9]

$$Q_{diff,q}\approx\frac{Q_{diff,q=1}}{q^2}. \qquad (5)$$

As the axial mode indices increases, the corresponding diffractive quality factor reduces by q^2 and it indicates the amount of power generation is reduces too that makes the generation of stable power over tunable band of frequencies challenging.

In the present work, as stated in section I, the RF interaction cavity designed for the 212 MHz DNP NMR spectroscopy applications is considered, the beam and geometrical parameters are given in Tables I and II [7]. The computations are made to determine the axial RF field profiles $V_{mp}(z)$, resonating frequencies and corresponding diffractive quality factors Q_{diff}, under beam absent conditions.

Table I: Design beam parameters of Colin D Joye *et al.*[7]

Parameter	Value
Frequency f	139.65 GHz
Output power P_{out}	> 10 W
Beam voltage V_b	12.3 kV
Magnetic field at the cavity B	5.06 to 5.12 T
Pitch factor α	1.6
Harmonic number, s	1
Beam current I_b	25 mA

Table II: RF Interaction cavity dimensions of Colin D Joye *et al.* [7]

Parameter	Value
Cavity radius R_c	3.48 mm
Down taper length L_d	5.5 mm
Down taper angle θ_d	1^0
Up taper length L_u	36.25 mm
Up Taper angle θ_{up}	2^0
Middle section Length L_c	28.25 mm
Resonant Frequency f_{res}	139.65 GHz
Diffractive quality factor Q_{diff}	6950

The normalized axial RF field profiles, for various possible axial modes of the design, q =1, 2, and 3 with resonant frequencies along radius profile $R(z)$ are shown in Fig. 3. The calculated and reported resonant frequencies as well diffractive quality factors for various axial mode indices are tabulated in Table III. Even though there was no mention about the existence of the axial mode index 3 but we observed the existence of it through our calculation and the corresponding details are tabulated also.

Table III: Tapered RF cavity parameters

Mode	Reported f_{res} (GHz)	Calculated f_{res} (GHz)	Reported Q_{diff}	Calculated Q_{diff}
TE_{031}	139.650	139.647	6950	6950
TE_{032}	139.870	139.841	1750	1750
TE_{033}	Not stated	140.241	Not stated	810

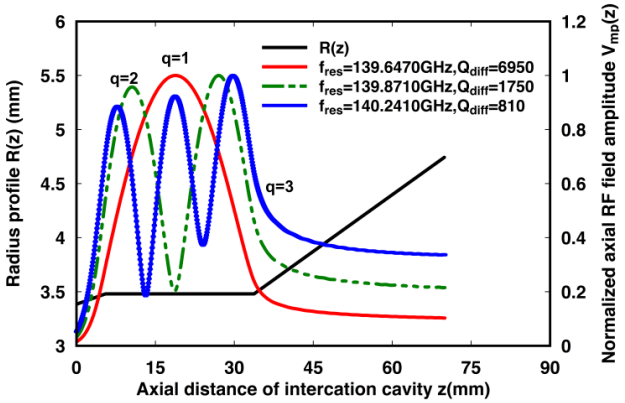

Fig. 3: Normalized cold cavity axial RF field amplitude profiles for various axial mode indices $TE_{0,3,q}$, where q=1,2,3 of Colin D. Joye *et al.*[7].

The possibility of oscillation of various modes in the cavity, subjected to the given beam parameters are assessed by calculating the start oscillation current curves I_{soc}. It is defined as the minimum amount of the current that allows mode to oscillate and grows significantly. Often, the beam current I_b is chosen greater than the I_{soc} currents of the desired operating mode for the oscillators. Apart from the oscillation of the mode, the mode competition information is also witnessed by allowing several modes in the calculation. The start oscillation current I_{soc} are calculated using linearized single-mode gyrotron theory and can be given as [3, 4]:

$$I_{start}(\Delta,\mu)=8.56\text{x}10^{4}\frac{\exp\left((\mu\Delta)^{2}/8\right)}{\mu^{2}\left(\mu^{2}\Delta-4s\right)}\frac{L_c\gamma_0}{Q\lambda}\left(\frac{\beta_{t0}^{2(3-s)}}{C_{mp}^{2}}\right) \quad , \qquad (6)$$

where C_{mp} is the coupling coefficient, and μ is normalized length of the interaction cavity, Δ is frequency mismatch or detuning parameter which are defined as [3-4]:

$$C_{mp}^{2}=\frac{J_{m\pm s}^{2}\left(\chi_{mp}R_b/R_c\right)}{\left(\chi_{mp}^{2}-m^{2}\right)J_{m}^{2}\left(\chi_{mp}\right)} \qquad (7)$$

$$\mu=\frac{\pi\beta_{t0}^{2}L_c}{\beta_{z0}\lambda} \qquad (8)$$

and

$$\Delta=\frac{2}{\beta_{t0}^{2}}\left(1-\frac{s\omega_{c0}}{\omega}\right) \quad . \qquad (9)$$

Here, s is the harmonic number that gives the relation between the operating frequency and the cyclotron frequency of electron beam provided by magnetic field, β_{t0} is the normalized transverse velocity at the entrance of the interaction region, ω_{c0} is the non-relativistic cyclotron frequency [3].

By varying the background DC magnetic field from 5 T to 5.2 T, the start oscillation current curves I_{soc} values for the operating mode $TE_{0,3,q}$ at various axial indices q are calculated for the Colin D Joyce *et al.* and plotted in Fig. 4. It is observed that, the minimum current required for oscillation of the TE_{03q}, at q = 1 and q = 2, is less than 20 mA, whereas for the q = 3 mode is above 35 mA. Since, the electron gun under consideration is limited to supply the beam current of maximum 25 mA. That can confirms the oscillation and thereby growth of the high order axial modes are unfeasible of mode $TE_{0,3}$ with q = 3 due to magnetic tuning and even for the excitation of q=2 mode is also challenging with given dimensions and beam parameters. Due to this limitation, the tuning of the device is achieved by changing the temperature of the coolant at the outer walls of the cavity thereby changes in the radius profile of the structure R (z) that affects the operating frequency.

It was mentioned that 0.2MHz/K has been observed as per thermal cooling technique. But if we are able to operate the device even in high order axial modes (q > 2), the tunable bandwidth of the device can be improved.

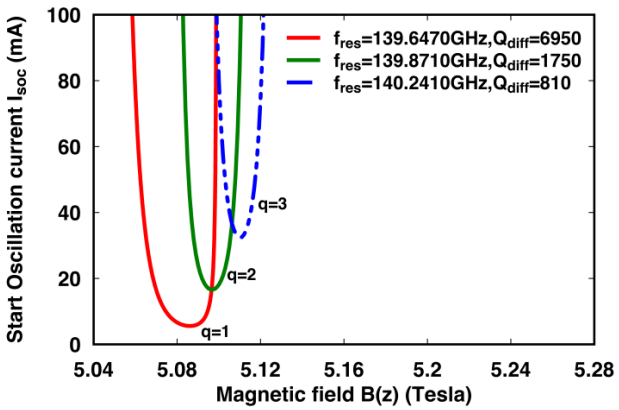

Fig. 4: Start oscillation current I_{soc} (mA) versus DC magnetic field B (Tesla) plots of $TE_{0,3,q}$ for different axial mode indices q of Colin D. Joye *et al.*[7]

Targeting the enhancement of the tunable bandwidth as the priority, the dimensions of the RF interaction cavity has been modified keeping the same beam parameters, such that the device is are able to operate in high order axial mode indices also. Considering the fact of longer cavities allows device to operate with low beam currents as well scope for exciting the high order axial modes by sacrificing the longer Q values. Since, the electron gun is limited of beam voltage 12.3 kV and beam current up to 25 mA, by modifying the cavity dimensions such that the device is able to operate for low beam currents I_b as well high axial mode operation.

The RF interaction cavity analysis is carried by considering various cavity geometrical combinations and the optimized modified dimensions are listed in Table IV. The corresponding RF characteristics namely, f_{res}, Q_{diff} of the various axial modes are tabulated in Table V and compared with characteristics of Colin D Joyce *et al* [7].

Table IV: Modified RF interaction cavity parameters

Modified cavity Parameters	Value
Cavity radius R_c	3.48 mm
Down taper length L_d	10.5 mm
Down taper angle θ_d	1^0
Up taper length L_u	36.25 mm
Up Taper angle θ_{up}	1^0
Middle section Length L_c	35.25 mm
Resonant Frequency f_{res}	139.62 GHz
Magnetic field B	5.05 -5.20 T

Table V: Resonating frequency f_{res} and diffractive quality factor Q_{diff} of modified cavity

Mode	Reported f_{res} (Ghz)	Calculated Q_{diff}
TE_{031}	139.62	10100
TE_{032}	139.771	2570
TE_{033}	140.0207	1152
TE_{034}	140.368	652

The cold cavity axial RF field profiles $V_{mp}(z)$ along with radius profile $R(z)$ of the modified cavity geometry are shown in Fig. 5. Assigning the same beam parameters, for the modified interaction cavity, the start oscillation current curves I_{soc} have been calculated over a range of magnetic fields B and are plotted in the Fig. 6. It has been observed that the minimum current required for the oscillation of the axial mode indices for q =1, 2 and 3 is less than 20 mA whereas for the axial mode q=4, it is at the verge of 25mA.

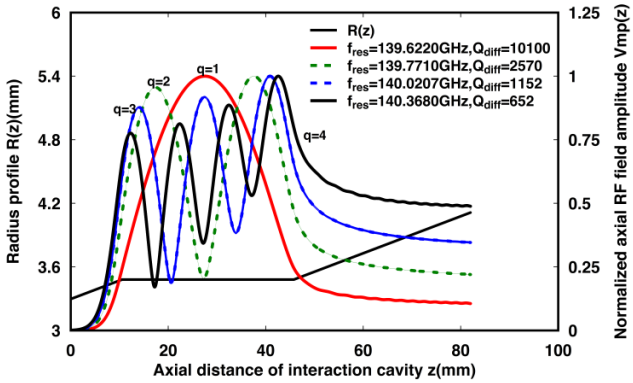

Fig. 5: Normalized cold cavity axial RF field amplitude profiles of modified cavities for various axial mode indices $TE_{0,3,q}$, for q=1,2,3,and 4.

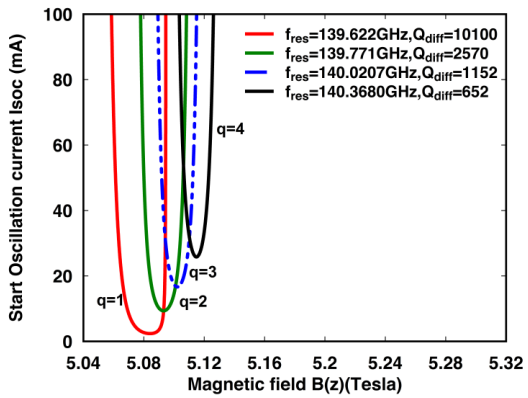

Fig. 6: Start oscillation current I_{soc} (in amperes) versus DC magnetic field B in (tesla) plots for different axial operating modes of $TE_{0,3,q}$ for modified RF cavity dimensions.

From the curves, it can be observed that the minimum values of I_{soc} are reduced as compared with Colin D Joye *et al.*, as well the excitation of axial mode index up to $q = 3$ is achievable since the minimum current required is well less than 25 mA. The longer interaction cavities allow more interaction space thereby chances of more electron beam and RF wave interaction results higher output power. These are examined by studying the beam wave interaction behaviour that gives information about the temporal growth of the RF power using time dependent multimode code theory as well performing the PIC simulation codes of commercially CST studio suite. The details of the electron beam-wave interaction studies for both the interaction cavities are carried and presented in detail Section III.

III. BEAM-WAVE INTERACTION EXPLORATION

With the beam parameter listed in Table I, for both RF interaction cavity geometries, the beam wave interaction mechanism has been studied using nonlinear multimode analysis given in various reports [8,9], as well by using a PIC solver code of commercially available CST studio suite. The beam wave interaction mechanisms have been carried for various beam parameters.

A. Time-dependent multimode analysis

A self-consistent time-dependent multimode nonlinear analysis developed by Fliflet *et al.* is used extensively for the study of the electron-beam and RF-wave interaction mechanism in the gyro devices [8]. In the present paper, a brief description of the procedure to follow for the beam wave interaction studies is explained as to analyze the beam-wave interaction behavior; starts with assumption of small mode amplitudes and random phases to a set of transverse electric modes. Then, solving the coupled, nonlinear, differential equations describing the electron phase and momentum equations over interaction length with small axial length steps along with the coupled time-dependent equations describing the mode phase and amplitude equations at each time step, and repeating it over the simulation time, for the determination of time varying behavior of various modes. Therefore, with the help of mode phases and amplitudes, the temporal growth of power levels in the possible operating modes and the corresponding electronic efficiency are calculated. The detailed procedure and the complete formulation used in the present study are extensively discussed in Fliflet *et al.* [8].

In the present study, selecting a uniform background DC magnetic field profile B(z) along the interaction length, the coupled equations are numerically integrated using fourth order Runge-Kutta method. A 12.3 kV DC voltage is applied to a uniformly distributed gyrating electron beam carrying a current of 25mA having 16 beamlets with 16 electrons in each beamlets. For the operating and its neighboring modes, like, $TE_{2,3}$, $TE_{0,2}$, the beam-wave interaction calculations are done. Taking various magnetic field values, the temporal growth of RF powers in the output mode for both the designs with respect to the time has been determined. The temporal growth of RF power in the main mode $TE_{0,3,1}$ for both the cavities are determined analytically and plotted in Fig.7. The RF powers of the operating modes for various magnetic fields are calculated while providing the axial mode index profiles with the corresponding frequencies for both the designs and are plotted in Fig. 8. For both cavities designs, the analytical calculations are carried out by taking the beam current around 25mA.

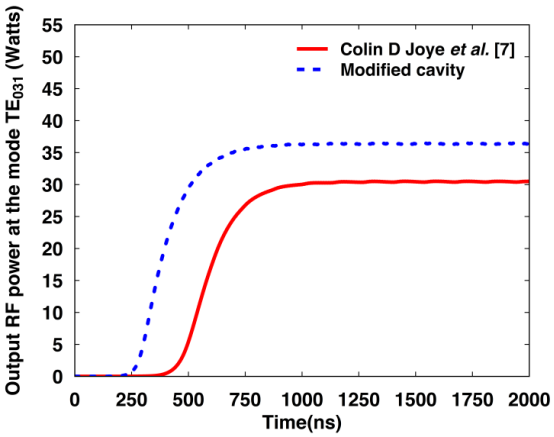

Fig. 7: Comparisons of RF power in the fundamental axial mode TE_{031} with respect to magnetic fields for cavities of Colin D Joye *et al.* [7] and modified design.

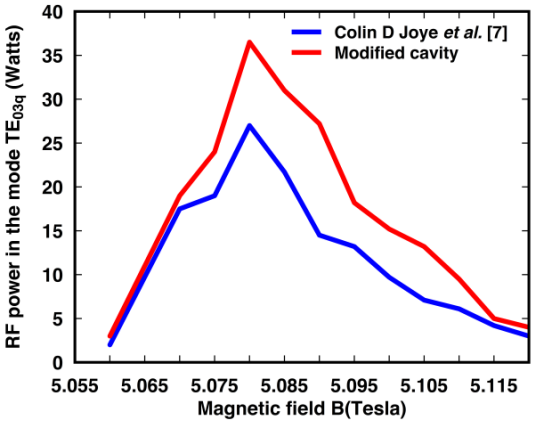

Fig. 8: Comparisons of RF power in the mode TE_{03q} with respect to magnetic fields for cavities of Colin D Joye *et al.* [7] and modified design.

B. PIC simulations of gyrotron

In addition to the non-linear multimode analysis, using 3D particle in cell solver, simulation of the electron beam and RF-wave interaction mechanisms of the device is performed reconfiguring a commercial code "CST Studio Suite" [10,11] for both the cavity geometries. A schematic modeled designed in CST studio suite selecting OFHC copper as the cavity material with conductivity of 2.9×10^7 S/m by assigning boundary conditions. A DC particle source is taken for forming the gyrating electron beam with assigned parameter, and magnetic field profile is applied along the device structure axis.

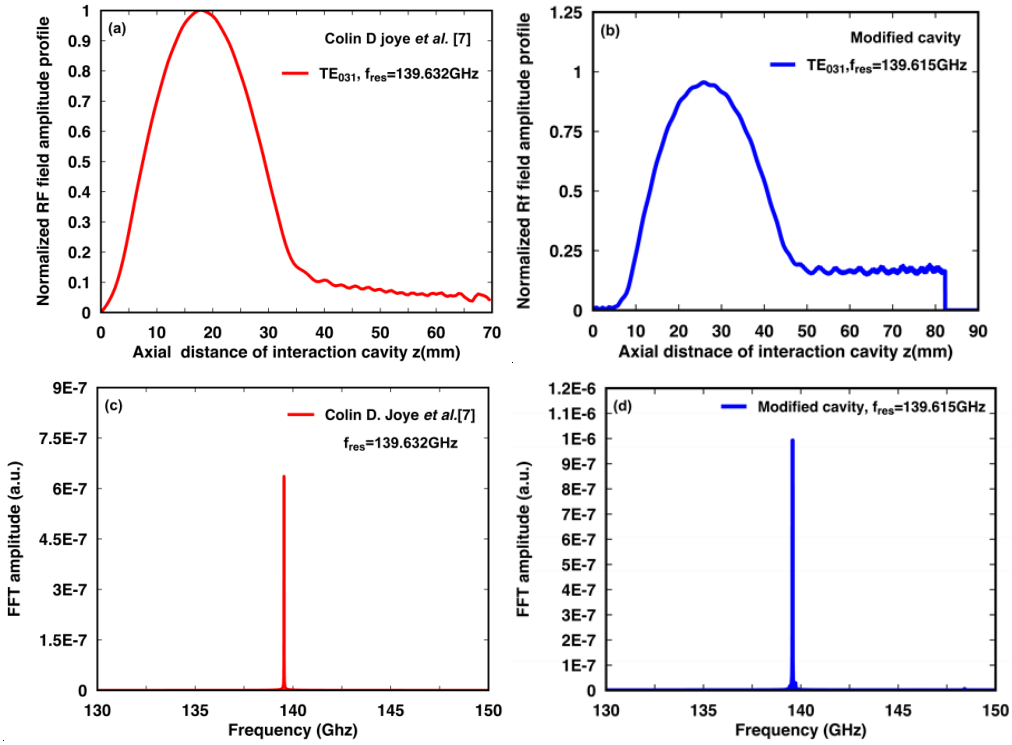

Fig. 9: PIC Simulation results-(a-b) hot axial RF field profiles (c-d)frequency response of the operating mode $TE_{0,3,q}$with axial index q=1 for cavities of Colin D Joye *et al*. [7] and modified designs respectively.

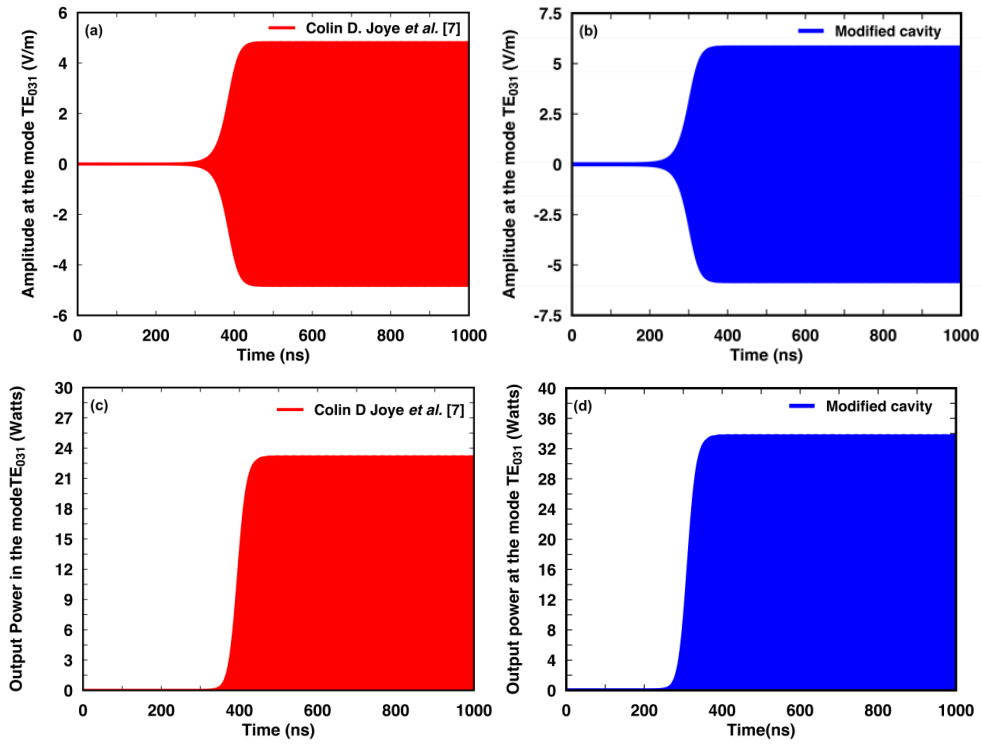

Fig. 10: PIC Simulation results- Temporal growth of mode TE_{031} (a-b) amplitudes (c-d) power values for cavities of Colin D Joye *et al*. [7] and modified designs respectively.

For observing the time varying behaviour of modes, various 3D E-field and H-field monitors are placed with suitable boundary conditions. The PIC simulation has run for 1000 ns and after the simulation time, by performing post processing steps, the necessary information for confirmation of the device design has been carried out.

The PIC simulated results for both the designs at beam current I_b=25mA and magnetic field 5.08T are shown in Figs. 9 and 10. The axial RF field profile in the presence of the electron beam along with fast Fourier transform of the mode is shown in Fig. 9. The temporal growth of mode amplitudes and the peak power generated in the mode $TE_{0,3,1}$ mode is shown in Fig. 10, It is found that the operating mode is oscillates at 139.630 GHz for the reported cavity dimensions and able to generate power of ~23W whereas for the modified cavity it has been observed that a stable RF power of more than ~27W oscillating at 139.590 GHz in the fundamental axial mode of TE_{031} for a beam current of 25mA at magnetic field 5.08T. Even an amount of more than 15W power is observed in the second axial mode index of $TE_{0,3,2}$ oscillating at 139.762 GHz for beam current of 25mA at magnetic field of 5.11T. By operating the device in the high order axial modes, through magnetic tuning, the operating bandwidth has been enhanced.

IV. CONCLUSIONS

A low power, tunable gyrotron operating in a $TE_{0,3,q}$ mode for 140 GHz DNP NMR spectroscopy applications is explored to facilitate wider bandwidth with magnetic tuning. The RF interaction cavity design, its beam absent RF characteristics as well as beam present RF wave interaction behavior, both analytical and Particle-in-Cell (PIC) simulation studies are presented. Gyrotron beam-wave interaction behaviour explored using time dependent non-linear multi-mode analysis for various beam currents and magnetic fields and more than >15W of RF power over a tunable bandwidth of 400MHz has been achieved through magnetic field tuning for the tailored the interaction cavity. More than 15W RF power output over a band of 400 MHz through magnetic tuning has been attained solely apart from thermal tuning at beam currents of around 25 mA. The thermal tuning behaviour for the modified cavity is yet to analyze. In addition, a 3D PIC simulation for fundamental modes TE_{031}, at beam currents 25mA for both the designs are carried out and found that the modified design gives more power compared with reported design due to lengthy interaction space. It is observed that, the time required for the growth of RF power gets reduced for the modified cavity. This tunable bandwidth gyrotron design provides immense use for the enhancement of sensitivity of the DNP NMR spectroscopy.

REFERENCES

1. M. Thumm, State-of-the-Art of High Power Gyro-Devices and Free Electron Masers. Update 2017 (KIT Scientific Reports; 7750). KIT Scientific Publishing, Vol. 7750, (2018).
2. G. S. Nusinovich, M. K. Thumm, and M. I. Petelin, “The gyrotron at 50: Historical overview,” Journal of Infrared, Millimeter, and Terahertz Waves, Vol. 35, no. 4, pp. 325–381, (2014).
3. C. Edgecombe, Gyrotron Oscillators: Their Principles and Practice (CRC Press, 2014).
4. B. Danly and R. J. Temkin, “Generalized nonlinear harmonic gyrotron theory,” The Physics of fluids, Vol. 29, no. 2, pp. 561–567, (1986).
5. M. K. Hornstein, “Design of a 460 GHz second harmonic gyrotron oscillator for use in dynamic nuclear polarization,” Diss. Massachusetts Institute of Technology, 2001. (https://dspace.mit.edu/handle/1721.1/86777)
6. A. C. Sousa “Frequency-tunable second-harmonic submillimeter-wave gyrotron oscillators,” Diss. Massachusetts Institute of Technology, 2010.(https://dspace.mit.edu/handle/1721.1/62463)
7. C. D. Joye, R. G. Griffin, M. K. Hornstein, K. N. Hu, K. E. Kreischer, M. Rosay, M. A. Shapiro, J. R. Sirigiri, R. J. Temkin RJ, P. P. Woskov, “Operational characteristics of a 14-W 140-GHz gyrotron for dynamic nuclear polarization,”. IEEE Transactions on Plasma Science. Vol. 34, no. 3, pp.518-23 (2006).
8. A. Fliflet, R. Lee, S. Gold, W. Manheimer, and E. Ott, “Time-dependent multimode simulation of gyrotron oscillators,” Physical Review A, Vol. 43, no. 11, p. 6166, (1991).
9. M. V. Kartikeyan, A. Kumar, S. Kamakshi,P. K.Jain,S. Illy, E. Borie ,B. Piosczyk, M. K.Thumm, “RF behavior of a 200-kW CW gyrotron,” IEEE Transactions on Plasma Science., Vol. 36, no.3, Jun pp.631-6(2008).
10. A. Singh, B. Ravi Chandra, and P. K. Jain, “Multimode behavior of a 42 GHz, 200 KW gyrotron,” Progress In Electromagnetics Research, Vol. 42, pp. 75–91, (2012).
11. User's Manual, CST-Particle Studio, Darmstadt, Germany, 2016.
12. B. Numerov, "Note on the numerical integration of d2x/dt2= f (xt)." *Astronomische Nachrichten* 230 (1927): 359.

AUTHORS PROFILE

Sivavenkateswara Rao V received the B.Tech. degree in electronics and communication engineering from JNTU, Hyderabad, India, in 2008, and the M.Tech. Degree in digital systems from MNNIT Allahabad, India, in 2012. He is currently pursuing the Ph.D. degree in microwave vacuum electron beam devices from IIT (BHU) Varanasi. His current research interests include digital image processing, beam-wave interaction and thermal studies of high power gyrotrons as well optimization techniques.

Muthiah Thottappan (M’14) received the Ph.D. degree in microwave engineering from IIT Varanasi, Varanasi, India, in 2013. He is currently an Assistant Professor with the Department of Electronics Engineering, IIT (BHU) Varanasi. His current research interests include RF & Microwave Engineering, High Power Microwave (HPM) Devices.

Pradip Kumar Jain (SM’05) received the B.Tech. degree in electronics engineering and the M.Tech. and Ph.D. degrees in microwave engineering from IIT (BHU) Varanasi, Varanasi, India, in 1979, 1981, and 1988, respectively. He is currently a Professor with the Department of Electronics Engineering, IIT Varanasi. His current research interests include High Power RF / Microwave Devices, Circuits and Systems. RF MEMs, Metamaterial devices Microwave Imaging and Remote Sensing.